

# Properties of the Young Milky Way Globular Cluster Whiting 1 from Near-Infrared Photometry

A. T. Valcheva<sup>1\*</sup>, E. P. Ovcharov<sup>1</sup>, A. D. Lalova<sup>2</sup>, P. L. Nedialkov<sup>1</sup>, V. D. Ivanov<sup>3</sup> and G. Carraro<sup>3</sup>

<sup>1</sup>*Department of Astronomy, University of Sofia, 5 James Bourchier Blvd., Sofia 1164, Bulgaria*

<sup>2</sup>*Institute of Optical Materials and Technologies, Bulgarian Academy of Sciences, 109 Acad. G. Bontchev Str., 1113 Sofia, Bulgaria*

<sup>3</sup>*European Southern Observatory, Ave. Alonso de Cordova 3107, Casilla 19, Santiago 19001, Chile*

Accepted 2014 October 9. Received 2014 October 9; in original form 2013 December 26

## ABSTRACT

Whiting 1 is a member of the fast-growing group of young globular clusters in the Milky Way halo. Preliminary estimates of its fundamental parameters have been provided using optical photometry and low resolution spectroscopy. In an attempt to strengthen our knowledge of Whiting 1, in this study we employ a complementary approach. Isochrone fitting method was applied on the Near-Infrared Color-Magnitude Diagram and yields an age  $t=5.7\pm0.3$  Gyr, metallicity  $z=0.006\pm0.001$  ( $[\text{Fe}/\text{H}]=-0.5\pm0.1$ ) and distance modulus  $(m-M)_0=17.48\pm0.10$ . Our results confirm that Whiting 1 is a young and moderately metal-rich globular cluster. It is one of the youngest from the Sgr dSph. We fitted an Elson, Fall and Freeman (EFF) profile to the near-infrared number counts, and measured cluster core radius  $r_c=9.1''\pm3.9''$ . Two probable eclipsing variables in the cluster were found from multi-epoch  $V$  band photometry. Finally, an unknown galaxy cluster was identified on our  $K$  vs.  $(J-K)$  color-magnitude diagram. It has a redshift  $z\sim1$ , and it is located at about  $1'$  from the center of Whiting 1 at  $\alpha_{J2000} = 02^h02^m56.6^s$ ,  $\delta_{J2000} = -03^\circ16'09''$ , contaminating the cluster photometry.

**Key words:** Galaxy: globular clusters: general – Galaxy: globular clusters: individual: Sgr dSph – Galaxy: globular clusters: individual: Whiting 1 – Galaxies: clusters: general – Galaxies: clusters: individual: Cl J020256.6-031609

## 1 INTRODUCTION

Whiting 1 ( $\alpha_{J2000} = 02^h02^m57^s$ ,  $\delta_{J2000} = -03^\circ15'10''$ ) is a halo globular cluster at a heliocentric distance  $D\sim45$  kpc, as first shown by Carraro (2005). It was discovered by Whiting et al. (2002) during a search for Galaxies in the Zone of Avoidance, and originally it was classified as an open cluster by Dias et al. (2002). Later, Carraro et al. (2007) confirmed its association with the Milky Way halo with deep  $BVI$  photometry, and updated the heliocentric distance to  $D\sim29.4$  kpc. They derived an age of 6.5 Gyr and metallicity  $z=0.004\pm0.001$  from isochrone fitting and estimated  $A_V=0.11$  mag and  $(m-M)_0=17.34$ . In latter study, measured  $\text{CaII}$  indexes ( $\Sigma\text{CaII}$ ) of three stars in Whiting 1 give metallicity  $[\text{Fe}/\text{H}]$  ranging from  $-1.1$  to  $-0.4$  ( $z$  ranging from 0.002 to 0.008). They pointed out that Whiting 1 is spatially close to the trailing stream of Sgr dSph, and its kinematics is consistent with that of this galaxy. Besides, it follows very nicely the Sgr dSph age-metallicity relation (Forbes et al. 2004; Siegel et al. 2007).

Only a few globular clusters in the halo of the Galaxy are known to have comparably young ages (*i.e.*, Pal 1 – Rosenberg et

al. 1998a; Pal 12 – Rosenberg et al. 1998b; Segue 3 – Ortolani et al. 2013; Crater – Belokurov et al. 2014), making Whiting 1 a member of a rare class of objects.

Up to now no NIR photometry of Whiting 1 has been reported in the literature and in this study we aim to obtain the fundamental properties through the NIR CMD using data from the ESO Science Archive<sup>1</sup>. Also, a search for variable star population has never been performed.

The next section describes our data. Section 3, 4 and 5 present our analysis and results of the NIR data: cluster structural parameters and cluster fundamental parameters - age, metallicity and distance modulus. Section 6 describes our search for variable stars in  $V$  band and our conclusions are drawn in Section 7.

## 2 OBSERVATIONS AND DATA REDUCTION

### 2.1 NIR observations

Whiting 1 was observed in the NIR on 2006 September 4 at the ESO NTT (New Technology Telescope) with SofI (Son of

\* E-mail: valcheva@phys.uni-sofia.bg

<sup>1</sup> <http://archive.eso.org>

ISAAC; Moorwood et al. 1998) in large-field imaging mode. Sofi is equipped with a 1024×1024 detector, with a pixel scale of 0.292 arcsec pix<sup>-1</sup> and FOV of 4'.98 × 4'.98. We had 15 images in  $J_S$  (each was the average of 4 frames of 15 sec integration) and 32 images in  $K_S$  (each was the average of 6 frames of 10 sec integration). The seeing during the observations was 0''.8 – 0''.9 on average for both filters. The data reduction was carried out with IRAF<sup>2</sup>, and included flat fielding, sky/bias/dark subtraction, image alignment and combination. The sky frame was created by median combination of all images with the task *imcombine*, applying the *avsigclip* 3- $\sigma$  rejection algorithm, and appropriate thresholds to excise the stars. A constant was added to the sky subtracted images during the final combination to set their median value to zero, accounting for the sky variations during the observations. Next, we performed PSF photometry (Stetson 1987) with DAOPHOT/IRAF. Only 99 stars were measured in both  $J_S$  and  $K_S$ . The 100% completeness limits were defined from the first drop in the luminosity function which give  $J_S^{lim} \sim 19.5$  mag and  $K_S^{lim} \sim 18.2$  mag (magnitude bins varied from 0.1 to 0.3), and the photometric errors for stars brighter than these limits are typically less than 0.1 mag. The photometric calibration was based on 9 stars for  $J_S$ , and 7 stars for  $K_S$ , in common with the Two Micron All Sky Survey (Skrutskie et al. 2006, 2MASS).

$$J = j_s - 2.208(\pm 0.019), \quad (1)$$

$$K_S = k_s - 2.894(\pm 0.023), \quad (2)$$

where the lower case letters mark the instrumental magnitudes, and the upper case ones mark the standard magnitudes (hereafter we will use the designation K for  $K_S$  filter).

## 2.2 Optical Variability Monitoring

Optical images of Whiting 1 were collected with EMMI (ESO Multi-Mode Instrument; D'Odorico 1990) and EFOSC2 (ESO Faint Object Spectrograph and Camera; Snodgrass et al. 2008) on the 3.58-m ESO NTT (New Technology Telescope) at La Silla, Chile, typically to fill small gaps in other programs or during periods of poor weather conditions. Binning by a factor of two was used on all occasions, making the pixels scales 0.33 and 0.24 arcsec pix<sup>-1</sup> and the FOV 5'.6 × 9'.9 and 4'.1 × 4'.1, respectively for both instruments. Five epochs were obtained in  $V$  band, and the first was paired with  $I$  band for quasi-simultaneous color information. The total integration for each epoch was split into three images, taken with some offsets to minimize the effects from the detector's cosmetics. A detailed log of the observations is presented in Table 1. The basic reduction was carried out with IRAF. For every epoch, we flat-fielded, aligned and co-added all images in the same filter. Next, we performed PSF photometry. The astrometric calibration is based on ten stars from Guide Star Catalog 2.3.2 (Lasker et al. 2008) and the photometric calibration is based on 210 stars we have in common with the catalog of Carraro et al. (2007). The derived photometric transformation equations are:

$$V_1 = v_1 + 1.921(\pm 0.012), \quad (3)$$

$$V_2 = v_2 + 1.849(\pm 0.012), \quad (4)$$

<sup>2</sup> Image Reduction and Analysis Facility is a general purpose software system for the reduction and analysis of astronomical data, IRAF is written and supported by the IRAF programming group at the National Optical Astronomy Observatories (NOAO).

**Table 1.** Log of the optical monitoring observations.

| Epoch No. | Date yyyy/mm/dd | UTC hh:mm:ss | Exp. [sec] | Instru-ment | Fil-ter | FWHM [arcsec] |
|-----------|-----------------|--------------|------------|-------------|---------|---------------|
| 1         | 2006/11/11      | 00:49:07     | 200        | EMMI        | V       | 1.0           |
| 1         | 2006/11/11      | 00:53:00     | 200        | EMMI        | V       | 0.85          |
| 1         | 2006/11/11      | 00:56:54     | 200        | EMMI        | V       | 1.0           |
| 1         | 2006/11/11      | 01:03:06     | 200        | EMMI        | I       | 1.0           |
| 1         | 2006/11/11      | 01:00:00     | 200        | EMMI        | I       | 1.0           |
| 1         | 2006/11/11      | 01:00:00     | 200        | EMMI        | I       | 1.0           |
| 2         | 2006/11/11      | 05:43:03     | 200        | EMMI        | V       | 0.85          |
| 2         | 2006/11/11      | 05:46:56     | 200        | EMMI        | V       | 0.83          |
| 2         | 2006/11/11      | 05:50:51     | 200        | EMMI        | V       | 0.83          |
| 3         | 2006/11/29      | 05:42:11     | 200        | EFOSC       | V       | 1.3           |
| 3         | 2006/11/29      | 05:46:18     | 200        | EFOSC       | V       | 1.3           |
| 3         | 2006/11/29      | 05:50:26     | 200        | EFOSC       | V       | 1.3           |
| 4         | 2006/12/18      | 02:52:19     | 200        | EFOSC       | V       | 0.8           |
| 4         | 2006/12/18      | 02:56:19     | 200        | EFOSC       | V       | 0.8           |
| 4         | 2006/12/18      | 03:00:19     | 200        | EFOSC       | V       | 0.8           |
| 5         | 2007/01/27      | 01:18:40     | 200        | EMMI        | V       | 1.65          |
| 5         | 2007/01/27      | 01:23:10     | 200        | EMMI        | V       | 1.65          |
| 5         | 2007/01/27      | 01:27:45     | 200        | EMMI        | V       | 1.65          |

$$V_3 = v_3 + 2.222(\pm 0.016), \quad (5)$$

$$V_4 = v_4 + 2.047(\pm 0.019), \quad (6)$$

$$V_5 = v_5 + 1.658(\pm 0.015), \quad (7)$$

$$I_1 = -0.09(\pm 0.20) + 1.11(\pm 0.01) * i_1, \text{ for } i_1 \leq 17 \text{ mag}, \quad (8)$$

$$I_1 = i_1 + 1.737(\pm 0.005), \text{ for } i_1 > 17 \text{ mag}, \quad (9)$$

where the lower case letters mark the instrumental magnitudes, and the upper case ones mark the standard magnitudes. The subscripts give the epoch number, as defined in Table 1. No significant color terms were found.

We cross-identified all photometry lists. For the first epoch 865 stars were measured in  $V$  and  $I$  bands simultaneously. There are 273 stars with three  $V$  band epochs, 259 star with four, and 231 with five. The EFOSC2's images are nearly two times smaller compared to EMMI's and the cluster is not centered in the EMMI's images. This highly reduces the number of common stars.

An excerpt of the photometric catalog is given in Table 2.

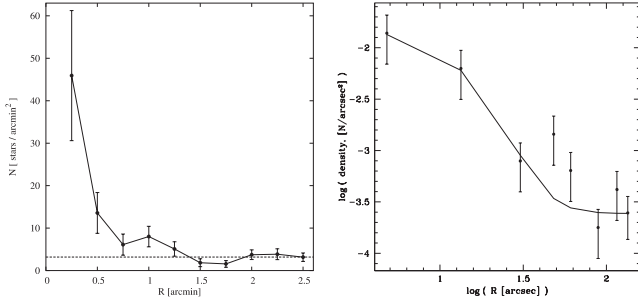
## 3 CLUSTER RADIUS AND STRUCTURAL PARAMETERS FROM THE NIR OBSERVATIONS

The wide field of view of our NIR images (4.92'×4.92') allows us to verify the cluster radius and structural parameters. The previous radius estimates range from 0'.5, obtained from the radial density distribution of stars (Carraro 2005), to 0'.6 - angular apparent radius (Dias et al. 2002). The deeper photometry of Carraro et al. (2007) suggests, based on a simple visual inspection, that the cluster may extent out to 1'.5. Carraro et al. (2007) fitted King's profile (King 1962) to obtain a core radius  $r_c=15''$ . This work showed an excess of stars in the outer region, approximated by a power law, attributed to tidal stripping.

We built a radial profile counting stars within 0.25' wide concentric annuli, centered on Whiting 1, and normalized them to unit area (Fig. 1, left). Throughout our analysis we used cluster center

**Table 2.** Photometry of the stars in Whiting 1 and the surrounding field. The complete catalogue is available online.

| N  | $\alpha_{J2000}$ | $\delta_{J2000}$ | $V_1$  | $\sigma(V_1)$ | $V_2$  | $\sigma(V_2)$ | $V_3$  | $\sigma(V_3)$ | $V_4$  | $\sigma(V_4)$ | $V_5$  | $\sigma(V_5)$ | $I_1$  | $\sigma(I_1)$ | $J$    | $\sigma(J)$ | $K_S$  | $\sigma(K_S)$ |
|----|------------------|------------------|--------|---------------|--------|---------------|--------|---------------|--------|---------------|--------|---------------|--------|---------------|--------|-------------|--------|---------------|
|    | hh:mm:ss         | dd:mm:ss         | mag    | mag           | mag    | mag           | mag    | mag           | mag    | mag           | mag    | mag           | mag    | mag           | mag    | mag         | mag    | mag           |
| 1  | 2:02:54.63       | -3:12:43.8       | 23.336 | 0.043         | 23.491 | 0.082         | 23.175 | 0.086         | 23.378 | 0.052         | 23.386 | 0.241         | 21.629 | 0.031         | 20.312 | 0.100       | 18.804 | 0.164         |
| 2  | 2:03:03.82       | -3:12:52.1       | 22.434 | 0.027         | 22.433 | 0.038         | 22.706 | 0.059         | 22.577 | 0.039         | 22.261 | 0.080         | 21.518 | 0.030         | 19.653 | 0.082       | 18.705 | 0.170         |
| 3  | 2:02:59.28       | -3:13:07.8       | 21.731 | 0.121         | 21.709 | 0.017         | 21.844 | 0.030         | 21.771 | 0.014         | 21.754 | 0.056         | 20.458 | 0.025         | 19.722 | 0.060       | 18.835 | 0.164         |
| 4  | 2:02:54.22       | -3:13:07.6       | 22.045 | 0.046         |        |               |        |               |        |               |        |               | 20.229 | 0.036         | 19.171 | 0.074       | 17.641 | 0.069         |
| 5  | 2:02:57.19       | -3:13:12.2       | 22.847 | 0.087         | 22.850 | 0.082         | 22.524 | 0.054         | 22.651 | 0.065         | 22.525 | 0.092         | 20.843 | 0.073         | 19.566 | 0.093       | 18.049 | 0.129         |
| 6  | 2:03:00.11       | -3:13:24.9       | 23.454 | 0.082         | 23.405 | 0.093         | 23.233 | 0.086         | 23.346 | 0.076         | 22.925 | 0.173         | 21.840 | 0.099         | 20.003 | 0.100       | 17.798 | 0.102         |
| 7  | 2:03:02.95       | -3:13:31.9       | 23.004 | 0.035         | 23.001 | 0.054         | 23.036 | 0.070         | 23.031 | 0.053         | 22.785 | 0.148         | 21.268 | 0.018         | 20.095 | 0.088       | 18.565 | 0.126         |
| 8  | 2:03:02.26       | -3:13:42.1       | 22.604 | 0.033         | 22.560 | 0.037         | 22.589 | 0.050         | 22.586 | 0.037         | 22.481 | 0.096         | 20.635 | 0.034         | 19.487 | 0.060       | 17.934 | 0.090         |
| 9  | 2:03:03.42       | -3:13:45.1       | 21.370 | 0.053         | 21.358 | 0.050         | 21.349 | 0.040         | 21.358 | 0.041         | 21.201 | 0.039         | 20.420 | 0.050         | 19.705 | 0.092       | 18.456 | 0.141         |
| 10 | 2:03:03.27       | -3:13:50.9       | 22.804 | 0.024         |        |               |        |               |        |               |        |               | 20.632 | 0.033         | 19.500 | 0.053       | 18.800 | 0.157         |


**Figure 1.** Left: Radial density distribution of all stars in the field in concentric rings around the cluster center with 0.25' bin. Contamination level, estimated at distance  $1.75' < r < 2.5'$ , is shown with dashed line. Error bars give Poisson uncertainties. Right: Elson, Fall & Freeman profile (Elson et al. 1987) fit to the observed radial profile. See Sect. 3 for the fitting parameters.

coordinates from Dias et al. (2002), cited in the introduction of this paper. The profile shows some excess counts over the background at  $r \sim 1' - 1.25'$  but we conservatively adopt a cluster radius of 0.75' for the following Color-Magnitude Diagrams (CMD) analysis, to minimize the field contamination. Our attempts to fit King's profile failed, possibly due to the small number of stars. However, we could fit Elson, Fall & Freeman's profile (hereafter EFF; Elson et al. 1987; Fig. 1, right):

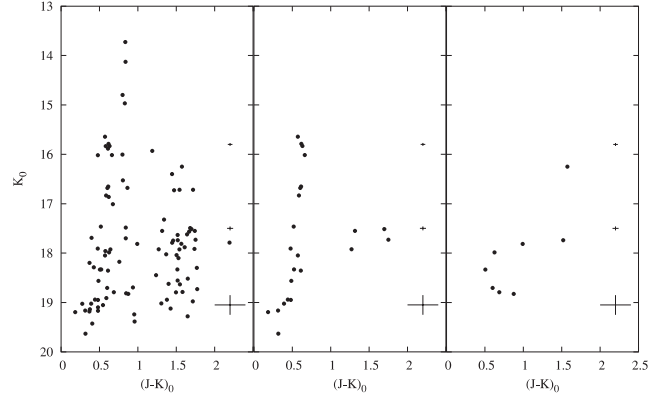
$$n(r) = n_0 \times (1 + r^2/a^2)^{-\gamma/2} + \Phi. \quad (10)$$

where  $n_0$  is central star-density,  $\gamma$  is power-law slope,  $\Phi$  is the background contamination level,  $a$  is a parameter, related to the core radius  $r_c$  via  $r_c = a \times (2^{2/\gamma} - 1)^{1/2}$ . We only considered stars with  $K_0 \leq 18.6$  mag and  $(J - K)_0 \leq 0.99$  mag to remove the bulk of background galaxies, and obtained:  $n_0 = 0.0153 \pm 0.0064$  stars/ $\square''$ ,  $\gamma = 5.27 \pm 1.53$ ,  $\Phi = 0.000244 \pm 0.000083$  stars/ $\square''$ ,  $a = 20.0'' \pm 4.0''$ ,  $r_c = 9.09'' \pm 3.68''$ . Our NIR core radius is similar to the optical value of Carraro et al. (2007).

#### 4 NIR COLOR-MAGNITUDE AND COLOR-COLOR DIAGRAMS

CMDs for Whiting 1 and the surrounding field are shown in Fig. 2, and a comparison of probable cluster members, defined to lie within 0.75' from the cluster center with an equal area background field.

The cluster members occupy a locus at  $(J - K)_0 \sim 0.3 - 0.7$  mag and  $K_0 \sim 15.5 - 19.5$  mag (Fig. 2, center). The faintest cluster stars


**Figure 2.** CMDs for all stars in the observed field (left), for the “cluster” stars within 0.75' from the cluster center (middle), and for stars in a control ring at  $r=2'$  with an area equal to the “cluster” area. Typical errors for stars with  $(J - K)_0 \sim 0.5$  mag are shown on the right. Extinction correction for  $E(J - K) = 0.013$  mag (Schlegel et al. 1998) is applied to all stars.

we detected are sub-giants at  $K_0 \sim 18.7 - 19.5$  mag. The extremely red objects at  $(J - K)_0 \sim 1.3 - 1.7$  mag and  $K_0 \sim 17.5 - 18$  mag probably belong to the field, as suggested by the right panel in Fig. 2 and by the Besançon model of stellar population synthesis of the Galaxy (Robin et al. 2003), which predicts only 2 foreground stars between 15 mag and 18 mag in  $K$  band in the cluster's field ( $r = 0'.75$ ). The expected number of stars for the whole imaged field predicted by Besançon model is 25 stars in the magnitudes interval [13-20] mag.

The CMD of all stars in the field (Fig. 2, left) has an abundance of sources with  $(J - K)_0 \geq 1.2$  mag, possibly distant galaxies (Fig. 3). Indeed, their colors are consistent with those of GALEV evolutionary synthesis models (Kotulla et al. 2009) for E/Sa galaxies at  $z \sim 1$  (Fig. 3, left). The spatial distribution of the sources showed some clustering of sources with  $J = 19 - 20$  mag and  $(J - K)_0 \sim 1.6$  mag within a circle with  $\sim 1.5'$  diameter at  $\alpha_{J2000} = 02^h 02^m 56.6^s$ ,  $\delta_{J2000} = -03^\circ 16' 09''$ . This may be an unknown galaxy cluster: the NASA Extragalactic database<sup>3</sup> identified four galaxies with unknown redshift within 2' from Whiting 1; the nearest galaxy cluster reported by Wen et al. (2012) in their catalog of SDSS-III clusters is  $\sim 10.5'$  away, and it has photometric redshift  $z \sim 0.49$ . Finally, the bluer field objects with  $(J - K)_0 \leq 1.2$  mag appears to be dwarf stars,

<sup>3</sup> This research has made use of the NASA/IPAC Extragalactic Database (NED) which is operated by the Jet Propulsion Laboratory, California Institute of Technology, under contract with the NASA.

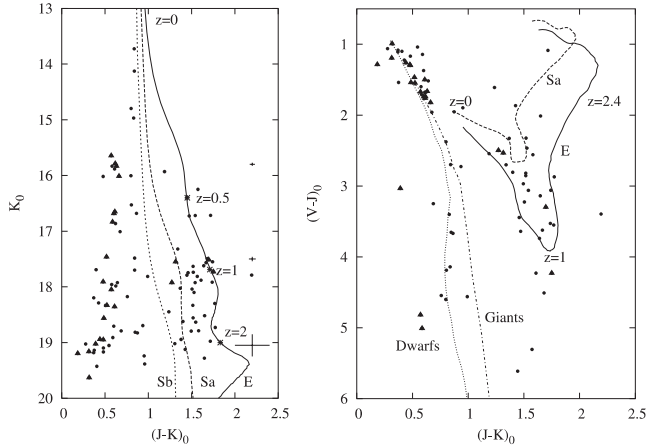


**Figure 3.** **Left:** Dereddened NIR CMD of all sources in the field ( $4.92' \times 4.92'$ ). The lines are GALEV models (Kotulla et al. 2009) for E (solid), Sa (dashed) and Sb (dotted) type galaxies, over cosmological timescales. Redshifts  $z$  are marked. Typical error bars for stars with  $(J-K_0) \sim 0.5$  mag are shown on the right. **Right:** Dereddened optical-NIR color-color diagram. GALEV models (Kotulla et al. 2009) for E (solid line) and Sa (dashed line) type galaxies, are shown, together with dwarfs (dotted line) and giant (dot-dashed line) star sequences from Frogel et al. (1978). **In both panels:** Candidate member stars (within  $0.75'$  from the cluster center) are marked with solid triangles, other sources are plotted with solid dots.

as seen from the right panels in Fig. 3 where we compare their location with the colors of dwarfs and giant stars (Frogel et al. 1978).

## 5 FUNDAMENTAL PROPERTIES VIA ISOCHRONE FITTING

We fitted the CMD of stars within  $0.75'$  radius from the Whiting 1 center with Padova PARSEC v1.1 isochrones (Bressan et al. 2012). We varied the metallicity  $z$  from 0.001 to 0.01 with a step of 0.0001 (91 different values) and the age  $t$  from 4.77 Gyr to 7.94 Gyr with a step  $\Delta(\log t) = 0.001$  ( $\sim 10$  Myr) (221 different values). Constant extinction of  $E(J-K) = 0.013$  mag (Schlegel et al. 1998) was applied to all stars. We kept the reddening constant because it is not expected to vary significantly at that Galactic latitude, and it has a small effect in the NIR.

We minimized  $\chi^2$  for each  $(z, t)$  pair treating the distance modulus  $(m-M)_0$  as a free parameter. The resulting  $\chi^2$  map is shown in Fig. 4, left panel. The relatively low values of the  $\chi^2$  ( $\sim 3$  near the minimum) compared to the number of the degrees of freedom (17) indicates an overestimation of the photometric errors. A parabolic fit was applied to the minimal values of  $\chi^2$  as a function of  $t$  and the minimum suggested a preferred value of  $t = 5.7 \pm 0.3$  Gyr. For the obtained  $t$ , the  $\chi^2$  as a function of the metallicity gives  $z = 0.0063 \pm 0.0011$ , again after fitting a parabola.

Finally, the best fitting distance modulus was  $(m-M)_0 = 17.48 \pm 0.10$ . The error includes both parametric (from the variation of  $z$  and  $t$  within their errors) and statistical (from the  $\chi^2$  fit) error. The  $\chi^2$  as a function of the age  $t$  and the distance modulus  $(m-M)_0$  is shown in Fig. 4, right panel.

Our results are based on RGB and sub-giant stars because the NIR data do not reach the main sequence turn off point. The derived properties are consistent, within  $1\sigma$ , with the ones obtained in the optics (Carraro et al. 2007), despite the smaller number of stars on the NIR CMD than on the optical CMD.

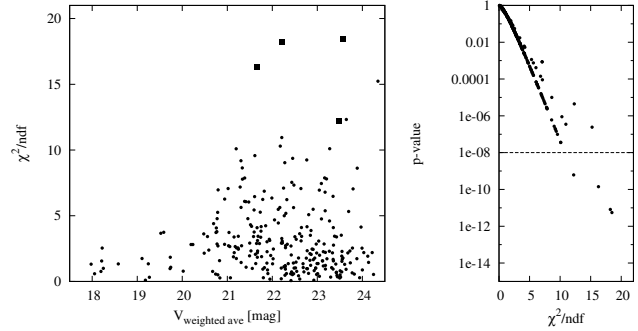


**Figure 5.** Diagrams  $\chi_n^2$  vs.  $V_{\text{weighted ave}}$  (left) and p-value vs.  $\chi_n^2$  (right) for all stars with three and more epochs in V band. P-values smaller than  $10^{-8}$  are adopted as a criteria for selection of candidate variables. The four candidates are marked with solid squares in the left panel.

## 6 SEARCH FOR VARIABLE STARS

We used our multi-epoch V band observations to search for variable stars in Whiting 1 and the surrounding field. We considered only the stars with three and more epochs - 273 stars in total. Because of the small number of measurements and different data quality for every star, we used normalized  $\chi^2$  and p-values (the probability to obtain these data if the available magnitudes for every star are randomly distributed around the mean value) to select candidates for variable stars. Diagram  $\chi_n^2$  vs.  $V$  is shown on the left panel in Fig. 5. Large dispersion is visible and expected, but some stars show extremely high values of  $\chi_n^2$  and can be potential variable candidates ( $\chi_n^2 > 12$ ). To check the significance of this selection, we calculated the p-value of every  $\chi_n^2$  (Fig. 5, right panel). The three visible sequences are stars with 3, 4 and 5 epochs. We considered as candidates variables only those with p-value smaller than  $10^{-8}$ , where we have something like a discontinuity in the diagram. The four selected stars are also marked on the left panel with solid squares.

After careful examination of the four selected candidates, we found that: the magnitude of the star #491 (the number in our photometric catalog) is affected by a cosmic ray; the star #363 is most probably the galaxy SDSS J020307.30-031501.0, which is at a distance of  $0.95''$  away from #363; the remaining two stars - #359 and #834 - exhibit statistically significant variability and both lie within the adopted cluster limits. They are marked in Fig. 6 with circles and their properties are listed in Table 3.

The differential light curves (Fig. 7) of the candidate variables #359 and #834 were generated with respect to the reference stars #672 and #851 which are the nearest stable stars similar in magnitude and color. The maximum peak-to-peak variation of both candidates is  $\sim 0.2$  mag over the monitoring period of 35 days with available data for 4 epochs.

We plotted all 273 stars with three and more epochs in V band on CMD  $V$  vs.  $V-I$  (see Fig. 8). Here, we used  $VI$  magnitudes from the first epoch. We selected the stars that lie within the determined cluster radius and one can see on the diagram that the cluster members mainly represent the lower part MS population. More massive stars have already evolved from the MS and the TO-point is well visible at  $V \sim 20.8$  mag. Some RGB stars are also present. For comparison, we plotted isochrones of PARSEC v1.1 (Bressan et al. 2012), which are reddened with the proper extinction (see Fig. 8) to match the observed MS, TO-point, RGB and the clump. The used parameters are in consistence with the previously obtained ones. The two candidate variables (empty circles in the latter figure) lie

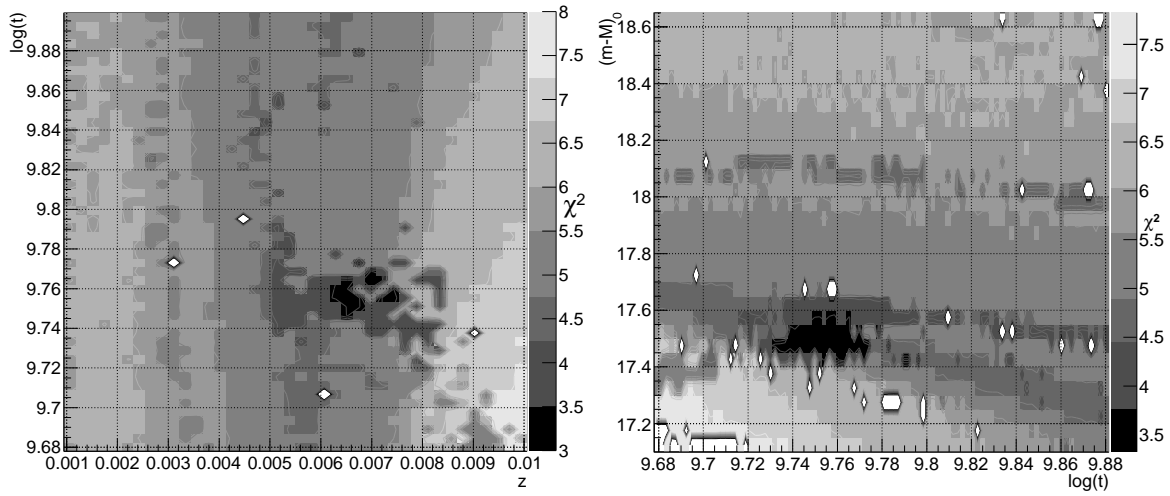


**Figure 4.**  $\chi^2$  as a function of: the metallicity  $z$  and the age  $t$  (left panel) and  $t$  and the distance modulus  $(m-M)_0$  (right panel). The white blocks show unsuccessful fitting.

**Table 3.** Candidate variable stars. Available  $V$  band epochs,  $I$  band, errors, computed  $\chi_n^2$  and p-values are listed.

| N   | $\alpha_{J2000}$<br>deg | $\delta_{J2000}$<br>deg | $V_1$<br>mag | $\sigma(V_1)$<br>mag | $V_2$<br>mag | $\sigma(V_2)$<br>mag | $V_3$<br>mag | $\sigma(V_3)$<br>mag | $V_4$<br>mag | $\sigma(V_4)$<br>mag | $I$<br>mag | $\sigma(I)$<br>mag | $\chi_n^2$ | p-value      |
|-----|-------------------------|-------------------------|--------------|----------------------|--------------|----------------------|--------------|----------------------|--------------|----------------------|------------|--------------------|------------|--------------|
| 359 | 2:02:57.47              | -3:14:59.2              | 21.540       | 0.017                | 21.518       | 0.022                | 21.751       | 0.031                | 21.685       | 0.018                | 20.865     | 0.034              | 16.281     | 1.408192e-10 |
| 834 | 2:02:56.75              | -3:14:59.2              | 22.151       | 0.018                | 22.160       | 0.027                | 22.090       | 0.054                | 22.343       | 0.020                | 21.332     | 0.032              | 18.218     | 8.141098e-12 |

in the middle and in the upper part of the MS but their luminosities are not high enough to suspect them neither as  $\delta$  Scuti nor as even dimmer  $\gamma$  Doradus pulsating variables. According to the best fitting isochrones the masses of both stars are close to 1 solar mass and the detected amplitude variations about 2 tenths of magnitude within a time span of a month may be related to stellar eclipses by a companion star – a likely possibility, taking into account their position on the CMD. Another option is a rotational modulation by Sun-like spots – the variation study (Radick et al. 1998) among a sample of Sun-like stars reveals at least one object - HD 129333 – with similar amplitude. However, due to the sparsity of the available data any further clarification of the nature of the variability of these stars is not possible.

## 7 CONCLUSIONS

In an attempt to strengthen our knowledge of Whiting 1 we used NIR photometry and determined the physical parameters of Whiting 1. We fitted isochrones to  $K$  vs.  $(J - K)$  color-magnitude diagram and derived an age  $t = 5.7 \pm 0.3$  Gyr, metallicity  $z = 0.006 \pm 0.001$  ( $[Fe/H] = -0.5 \pm 0.1$ ) and distance modulus  $(m - M)_0 = 17.48 \pm 0.10$ . Our results confirm that Whiting 1 is a young and moderately metal-rich globular cluster. It is one of the youngest from the Sgr dSph.

In the NIR CMD, we noticed a clustering of objects at  $\alpha_{J2000} = 02^h 02^m 56.6^s$ ,  $\delta_{J2000} = -03^\circ 16' 09''$  with radius  $r \sim 1.5'$ , presumably a background galaxy cluster. We estimated a redshift and  $z \sim 1$  is based on a comparison with the colors of GALEV evolutionary synthesis models (Kotulla et al. 2009) for E/Sa galaxies.

Our multi-epoch  $V$  band monitoring led up to the discovery of two candidate variable stars within the cluster radius. Their differential light curves give maximum peak-to-peak variation of  $\sim 0.2$  mag for both candidates over the monitoring period of 35 days and taking in to account their position on the CMD diagram the stars are likely to be eclipsing binaries.

## ACKNOWLEDGMENTS

Authors would like to thank Venelin Kozuharov for his valuable help on fitting analysis and the anonymous referee for his/her constructive comments and suggestions that helped us to greatly improve to the paper. The data used in the publication were retrieved from the ESO Science Archive. They were obtained under program IDs: 59.A-9002(A), 59.A-9908(A), and 60.A-9013(A). This publication makes use of data products from the Two Micron All Sky Survey, which is a joint project of the University of Massachusetts and the Infrared Processing and Analysis Center/California Institute of Technology, funded by the National Aeronautics and Space Administration and the National Science Foundation.

## REFERENCES

- Belokurov V., Irwine M.J., Koposov S.E., et al. 2014, MNRAS, 441, 2124
- Bressan A., Marigo P., Girardi L., et al. 2012, MNRAS, 427, 127
- Carraro G., 2005, ApJ, 621, L61
- Carraro G., Zinn R., Moni Bidin C., 2007, A&A 466, 181

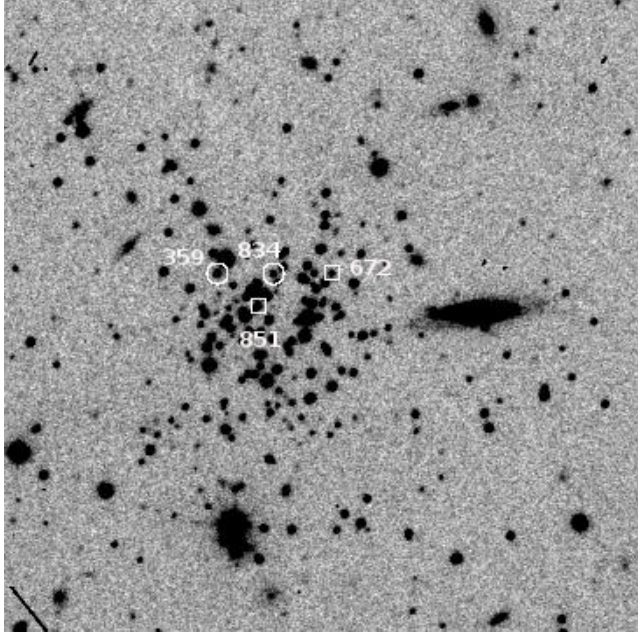


**Figure 6.** V band image of Whiting 1 (600 sec. of integration, 2'x2' FoV). Candidate variables are marked with circles and reference stars with squares. All stars are labeled with the corresponding number in our photometric catalog. North is up and East is to the left.

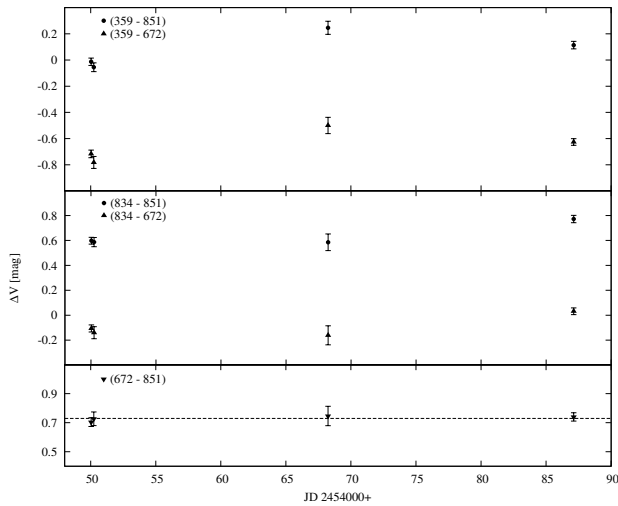


**Figure 7.** Differential light curves of the 2 candidate variables #359 and #834 and the reference stars #672 and #851 are presented on the top and middle panels. The difference between the reference stars #672 and #851 is shown on the bottom panel. Weighted average of the differences is plotted with dashed line.

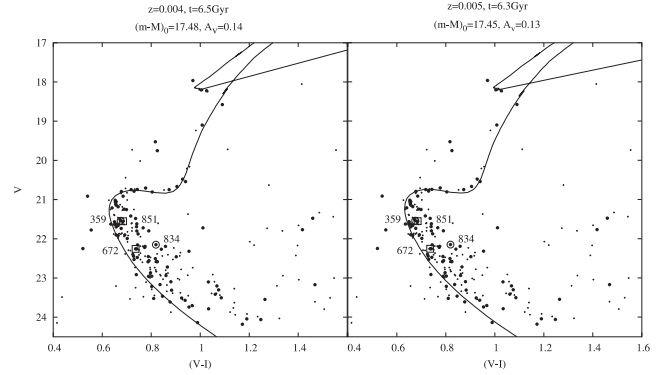


**Figure 8.** Optical color-magnitude diagram for all stars with 3 and more epoch in V band (crosses). Stars lying within the determined radius of 0.75' are shown with solid circles. No extinction correction is applied to the magnitudes. Two different isochrones are overlaid (their parameters are shown above each panel) and are reddened with the cited values. The two variable candidates #359 and #834 and the two reference stars #672 and #851 are marked with empty circle and empty squares, respectively.

369, 462

- Lasker B. M., Lattanzi M. G., McLean B. J. et al., 2008, *AJ*, 136, 735
- Moorwood A., Cuby J.-G., & Lidman C., 1998, *The Messenger* 91, 9
- Ortolani S., Bica E., & Barbuy B., 2013, *MNRAS*, 433, 1966
- Radick R. R., Lockwood G. W., Skiff B. A., & Baliunas S. L., 1998, *ApJS*, 118, 239
- Robin A.C., Reylé C., Derrière S., & Picaud S. 2003 *A&A*, 409, 523
- Rosenberg A., Saviane I., Piotto G., Aparicio A., & Zaggia S. R. 1998a, *AJ*, 115, 648
- Rosenberg A., Saviane I., Piotto G., & Held E. V. 1998b, *A&A*, 339, 61
- Schlegel D.J., Finkbeiner D.P., Davis M. 1998, *ApJ*, 500, 525
- Siegel M., Dotter A., Majewski S, et al. 2007, *ApJ*, 667, 57
- Skrutskie M.F., Cutri R.M., Stiening R., et al. 2006, *AJ*, 131, 1163
- Snodgrass C., Saviane I., Monaco L., & Sinclaire P. 2008, *The Messenger*, 132, 18
- Stetson P.B. 1987, *PASP*, 99, 191
- Wen Z.L., Han J.L., & Liu F.S. 2012, *ApJS*, 199, 34
- Whiting A.B., Hau G.K.T., & Irwine M. 2002, *ApJS*, 141, 123

This paper has been typeset from a  $\text{\LaTeX}$  file prepared by the author.

- Dias W.S., Alessi B.S., Moitinho A., & Lépine J.R.D., 2002, *A&A*, 389, 871
- D'Odorico S., 1990, *The Messenger*, 61, 51
- Elson R.A.W., Fall M.S., & Freeman K.C., 1987, *ApJ*, 323, 54
- Forbes D. A., Straden Y., & Brodies Y. P., 2004, *AJ*, 127, 339
- Frogel J.A., Persson S.E., Matthews K., & Aaronson M., 1978, *ApJ*, 220, 75
- King I., 1962, *AJ*, 67, 471
- Kotulla R., Fritze U., Weilbacher P. & Anders P., 2009, *MNRAS*,